An evaluation of six techniques for measuring porosity of ribbons produced by roller compaction

Yiwang Guo [1], Lizbeth Martinez [2], Arnesh Palanisamy [2], Bindhu Gururajan [2,3] and Changquan Calvin Sun [1,]*

[1.] Department of pharmaceutics, College of pharmacy, University of Minnesota, 308 Harvard St. S.E. Minneapolis, MN 55455

[2.] Novartis Pharma AG, Novartis Campus,Basel, 4056, Switzerland

[3.] School of Engineering, University of Edinburgh, Edinburgh, EH8 9YL, United Kingdom

**Corresponding author*

Changquan Calvin Sun, Ph.D.

9-127B Weaver-Densford Hall

308 Harvard Street S.E.

Minneapolis, MN 55455

Email: sunx0053@umn.edu

Tel: 612-624-3722

Fax: 612-626-212

Abstract

Ribbon porosity is a critical parameter to monitor in the roller compaction process. In this study, six techniques for measuring the porosity of solid compacts, i.e., manually by caliper (Caliper), X-ray microtomography (μCT), off-line near-infrared spectroscopy (NIR), laser triangulation (Laser), mercury intrusion porosimetry (MIP), and GeoPyc, were compared using a set of rectangular ribblets of microcrystalline cellulose (MCC). These ribblets, which were compressed at 8 - 130 MPa on a compaction simulator, exhibited porosities over the range of 0.09 – 0.52. Subsequently, porosities of MCC ribbons made on a roller compactor at specific roll forces of 1.8 kN/cm and 8.8 kN/cm were measured. The Caliper method is convenient for samples with a simple shape but not suitable for real ribbons. The accuracy of GeoPyc measurement relies on accurate conversion factor (unit in cm^3/mm), sample shape and size, and sufficient sample volume percentage in the medium. The μCT data is more accurate at lower porosities (< 0.2), while the MIP data is more accurate at higher porosities (> 0.4). The Laser method has good accuracy and is more reproducible compared to other methods in the ribblets measurement. The NIR method is fast, which makes it suitable for in-line monitoring of changes in ribbon quality, but porosity quantification is sensitive to sample presentation, such as surface curvature and roughness. These insights could assist in the choice of the most appropriate method for monitoring ribbon porosity to guide the development and optimization of a roller compaction process for a given formulation.

Keywords: roller compaction, ribbon density, porosity, Geopyc, laser triangulation, X-ray microtomography, mercury intrusion porosimetry, near-infrared spectroscopy.

1. Introduction

Ribbon porosity, ε, represents the fraction of voids in a specimen. It is a critical quality attribute (CQA) for ribbons produced in roller compaction (RC) because it directly affects the subsequent granule and tablet properties (Yu et al., 2014). Since ε is calculated from the knowledge of a solid sample density (ρ_{bulk}) and true density (ρ_{true}) using Eq. (1), ribbon density monitoring and control is an important consideration during scale-up (Boersen et al., 2016), processes transfer (Souihi et al., 2015), and modeling and simulations of a RC process (Nesarikar et al., 2012; Reimer and Kleinebudde, 2019).

$$\varepsilon = 1 - \frac{\rho_{bulk}}{\rho_{true}} \quad (1)$$

Where ρ_{bulk}/ρ_{true} is the solid fraction of the solid compacts, in which true density of the material, ρ_{true}, may be determined using different methods (Richards and Lindley, 2006), including calculation from single crystal structures (Elsergany et al., 2023), helium pycnometry (Chang et al., 2019), buoyancy method (Goldenberg et al., 2023), the Sun method (Sun, 2004), and in-die stress transmission method (Elsergany et al., 2023). The density of a solid sample, ρ_{bulk}, is calculated from sample mass, *m*, and envelop volume, *V*, (Eq. 2).

$$\rho_{bulk} = \frac{m}{V} \quad (2)$$

Since *m* can be accurately measured using a suitable analytical balance, ρ_{bulk} can be determined if *V* is known. Currently, several techniques are available for determining the *V* of samples, such as GeoPyc (Zinchuk et al., 2004), laser triangulation (Laser) (Lillotte et al., 2021), or caliper for samples with a simple geometry, e.g., rectangular (Keizer and Kleinebudde, 2020) or cylindrical tablets (Osei-Yeboah and Sun, 2015). Porosity can also be directly measured by mercury intrusion porosimetry (Khorasani et al., 2015a; Lu et al., 2000) or predicted from a measurable physical property based on a known calibration curve with density. The latter includes X-ray microtomography (μCT) (Mahmah et al., 2019; Miguélez-Morán et al., 2009), near-infrared spectroscopy (NIR) (Crowley et al., 2017a; Khorasani et al., 2015b; Lim et al., 2011), and terahertz spectroscopy (Bawuah et al., 2020; Zhang et al., 2016).

Each of these methods has its advantages and limitations in terms of accuracy, precision, sensitivity, measurement speed, ease of operation, sample preparation and amount, and capability for mapping. Thus, a suitable measurement method needs to be judicially selected according to application scenarios, such as at -, on -, or in - line process monitoring to overcome limitations of end product testing and to guide continuous manufacturing, or mapping to understand the density/porosity distribution inside a ribbon. In this study, six commonly used

techniques for measuring porosity of ribbons in the context of dry granulation were compared, including Caliper, GeoPyc, Laser, μCT, MIP, and off-line NIR methods, and both simulated ribbons (ribblets, a combination of the words ribbon and tablet) (Keizer, 2021)) from a compaction simulator and ribbons prepared using a roller compactor were used. To our best knowledge, there are similar studies, however with fewer number of techniques, such as comparing a laser triangulation technique to an oil intrusion method (Allesø et al., 2016), a laser triangulation technique to GeoPyc method and a manual caliper method (Iyer et al., 2014), terahertz imaging method to a section method where small pieces cut from a ribbon by a bandsaw was manually measured by a caliper (Zhang et al., 2016), and μCT method to laser triangulation technique and GeoPyc method (Lillotte et al., 2021). Along with these studies, this work is aimed at better understanding the pros and cons of these methods, and facilitates the selection of the most appropriate technique for ribbon porosity measurement to guide RC process development.

2. Materials and Methods

2.1. Materials

Microcrystalline cellulose (MCC, Avicel 105, International Flavors & Fragrances, Philadelphia, PA) was used as received.

2.2. Methods

2.2.1. Sample preparation

Ribblets were prepared by a uniaxial compaction simulator (Styl'One Evolution, MedelPharm, Beynost, France), using rectangular shaped flat faced tooling (16 × 9 mm). Ribblets were compressed at seven compaction pressures in the range of 8 - 130 MPa under a force control mode, resulting porosities covering a range of 0.09 - 0.52. The thickness of ribbons was maintained at ~3 mm by adjusting the weight of powder being compacted, i.e., ribblet dimensions were maintained at approximately 16 mm x 9 mm x 3 mm (Figure 1).

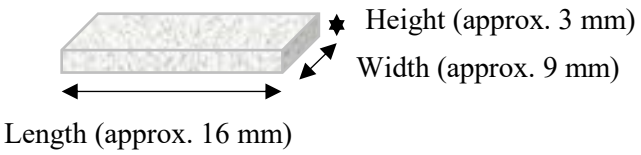

Figure 1. Schematic of a ribblet made by compaction simulator.

Real ribbons were prepared by a pilot-scale roller compactor (Alexanderwerk WP 120, Remscheid, Germany). A vertical feeding hopper discharged powder to a horizontal single screw

feeding system, which conveyed the powder forward into the compaction zone. The two counter-rotating rolls (knurled surface for upper roll and smooth surface for lower roll) were aligned vertically. The roll width (40 mm) and roll diameter (120 mm), roll speed (3.4 rpm), and roll gap (2.2 cm) were kept unchanged during the process. Two roll forces were applied to prepare ribbons with different porosities (~0.36 at 1.8 kN/cm and ~0.09 at 8.8 kN/cm). Ribbons were collected immediately after exiting the rolls after the machine reached a steady state.

2.2.2. Porosity measurement

Samples, either ribblets or ribbons, were stored for at least 48 hrs before porosity measurement. Six porosity measurement techniques were evaluated, among which, MIP measures sample porosity directly; NIR and μCT determine sample porosity through absorption spectra and gray value, respectively; while the Caliper, GeoPyc and Laser methods measure sample envelop density (ρ_{bulk}), which was used to calculate porosity using Eq. (1) with the true density value of 1.46 g/cm^3 for MCC (Sun, 2005).

2.2.3. Caliper method

A caliper (iGaging iP54 Fastener Cal Digital Calipers, CA, USA) with resolution of 0.01 mm was used to measure the length, width, and thickness of ribblets, which were used to calculate sample volume, *V*, and ρ_{bulk} by Eq. (2). The reported porosity at each pressure was a mean of the porosity from three independent samples. The Caliper method was not used to measure the porosity of real ribbons due to their bent shape and knurled surface pattern.

2.2.4. GeoPyc method

An envelope density analyzer (GeoPyc 1365, Micromeritics Inc., Norcross, GA) was used to measure envelop volume of ribblets or ribbons. This technique employs a dry powder medium (DryFlo), composed of micro-sized, nonhazardous, rigid spheres that do not fill sample's external or internal pores (Micromeritics, 2013). The GeoPyc measures sample volume change, before and after introducing a sample into the DryFlo medium. This was achieved by measuring the displacement of the piston in a glass cylinder with a constant inner diameter. For reliable results, about 4 g of sample (corresponding to 9 ribblets and ~25% of the final volume) were placed inside a bed of DryFlo in a glass cylindrical chamber with a diameter of 25.4 mm. The chamber was rotated and consolidated under a force of 51 N, and results were generated after 10 consecutive measurement cycles. The increase in volume over the sample-free DryFlo measured under the same condition was taken as sample volume. For each set of samples, measured volume was

used to calculate porosity (n = 3). Mean and standard deviation of measured porosity were calculated.

2.2.5. Laser triangulation technique (Laser)

A solid fraction analyzer (Solid Fraction Rapid Analyzer, V2, Solid Fraction Measurement Systems, Centerbrook, CT) was used to measure samples envelop volume based on laser triangulation technique, in which, a sample with certain size (Table 1) was scanned between dual opposed line-scan laser beams when moved on a computer-controlled translation stage to obtain sample volume. The entire volume of each sample was calculated by integrating thickness measurements over the sample surface on a 40 µm by 14 µm grid. Sample was then transferred to an internally equipped Mettler balance to determine sample mass. Based on the true density of the material input into the system, the solid fraction of the compacts was automatically calculated and displayed on the screen after each measurement (SolidFraction). Mean and standard deviation of porosity (= 1 - solid fraction) were calculated from three independent samples (n = 3).

2.2.6. X-ray microtomography (µCT)

Ribblets and ribbons were evaluated using a µCT machine (XT H 225, Nikon Metrology Inc., Brighton, MI, USA). The following parameters were used: 110 kV, 90A, 708 ms of exposure, 720 projections, 4 frames per projection, and a voxel size of 32 µm. The total image acquisition time was approximately 34 min for each run. 2D images were processed to reconstruct a three-dimensional image of the sample by CT Pro software (Nikon Metrology, Belgium). Visualization and analysis of the reconstructed 3D images was performed using the VG Studio 3.4 software (Volume Graphics GmbH, Germany). In each measurement, several pieces of ribblets or ribbons were stacked and scanned simultaneously. However, each sample was separately analyzed by selecting appropriate region of interest to determine porosity based on a previously established calibration curve (Figure S3). Three independent samples from each sample set were measured and the mean and standard deviation were calculated (n = 3).

The µCT method is a non-destructive method for measuring sample density, based on the attenuation of X-rays that pass through an object, i.e., intensity of the incident X-ray beam diminishes according to

$$I_x = I_0^{e^{-\mu x}} \qquad \text{Eq. (3)}$$

Where x is the distance of object to the source, I_x is the intensity of the beam after passing through the object at distance x, and μ is the linear attenuation coefficient, which is the product of

mass attenuation coefficient and sample density (Pawar, 2011). For a given material, the mass attenuation coefficient is constant, thus μ is linearly dependent on the sample density. The measure intensity I_x is a function of sample density, which is estimated by assuming a linear relationship between density and the degree of X-ray attenuation (Akseli et al., 2011; Sun et al., 2018), which is represented by gray value of the region of interest (Athanasiou et al., 2017). In this study, the linear relationship (Figure S3) between gray value and sample density was first established by a set of cylindrical MCC tablets prepared under a set of pressures. Porosity of the tablets was obtained through the Caliper method. During the image analysis, the entire tablet/ribblet was selected as the region of interest (ROI). Therefore, the measured porosity by μCT method in this work is the average value.

2.2.7. Mercury intrusion porosimetry (MIP)

A mercury intrusion pore size analyzer (Poremaster 60 GT, Anton Paar Switzerland AG) was used to measure ribbon porosity. A ribblet or ribbon sample was degassed under a 7 Pa vacuum before being immersed in mercury, which was subject to increasing pressures. The volume of mercury intruding into the sample as a function of pressure was measured. Pore size corresponding to each pressure was calculated according to Washburn's equation (Washburn, 1921). The total mercury intrusion volume above pore diameter of 0.003 μm (corresponding to an intrusion pressure of 400 MPa) was taken as porosity. Porosity values of of two separate samples from each set were averaged (n = 2). Unlike the four previously mentioned methods, MIP measures samples porosity directly. In this measurement, mercury intrudes into voids under pressure, with the pressure inversely proportional to the size of the pores (Berodier et al., 2016). Consequently, the volume of pores with a certain size could be estimated by measuring the additional volume of mercury intruding into a sample upon applying a higher pressure.

2.2.8. Near infrared spectroscopy (NIR)

Samples were placed in specially designed and 3D printed sample holders for collecting FT-NIR spectra in diffuse reflectance mode using an off-line MPA I spectrometer (Bruker Optik GmbH, Ettlingen Germany). Sample positioning for ribblets was relatively easy, since the surfaces of the ribblets were flat. However, it was difficult for real ribbons since they were slightly curved and one side had knurled pattern. To ensure good contact with the measuring window, only the flat side of the ribbon was evaluated. Samples were scanned over a spectral range of 12,000 to 4,000 cm^{-1} with a 16 cm^{-1} spectral resolution. Acquired spectra were analyzed using the software OPUS (Bruker Optik GmbH, Ettlingen Germany) and the average of 32 scans was reported. The

sampling spot had a diameter of 4.5 mm, corresponding to approximately an area of 16 mm^2. Each sample (n = 1) was scanned 6 times at the center with slight sample repositioning in between each measurement. Porosity from each scan was determined from a previously established calibration curve (Figure S5). The mean and standard deviation of each sample were calculated from the 6 measurements.

Since the NIR absorption of a material is affected by the density of the material being analyzed, it offers the potential of measuring the density/porosity of a solid compact. A higher NIR absorbance corresponds to a higher sample density and a lower porosity, following a linear relationship (Donoso et al., 2003; Khorasani et al., 2016). Similar to μCT, the NIR method requires the construction of a calibration curve (Figure S5). This was done by using ribblets (n=2 at each pressure) with a range of porosities measured by the Caliper method. Partial least squares (PLS) regression model was developed using spectral data in the 9403.8 cm^{-1} - 5538.9 cm^{-1} wavelength region. The accuracy of the PLS model was verified using a new set of ribblets.

3. Results and discussion

3.1. Ribblets from the compaction simulator

The initial comparison among the six methods was carried out using rectangular ribblets (Figure 1). Given that the volume of rectangular-shaped ribblets can be reliably determined by a caliper, the Caliper method was used as a reference for evaluating the accuracy of five other methods, i.e., GeoPyc, Laser, μCT, MIP, and off-line NIR methods (Figure 2).

Figure 2 summarizes orthogonal distance regression (ODR) analysis performed for data from each technique using SciPy (SciPy v1.6.2, Python v3.12.4). Standard deviations in both x and y were incorporated as weights for fitting except MIP, where standard deviations were not calculated since measurements were only duplicated (n = 2). The results indicate that all five methods led to porosity results well correlated with that from the Caliper method (Figure 2 a-e, Table S1). Specifically, estimates of the regressions (Figure 3) showed that GeoPyc provided both

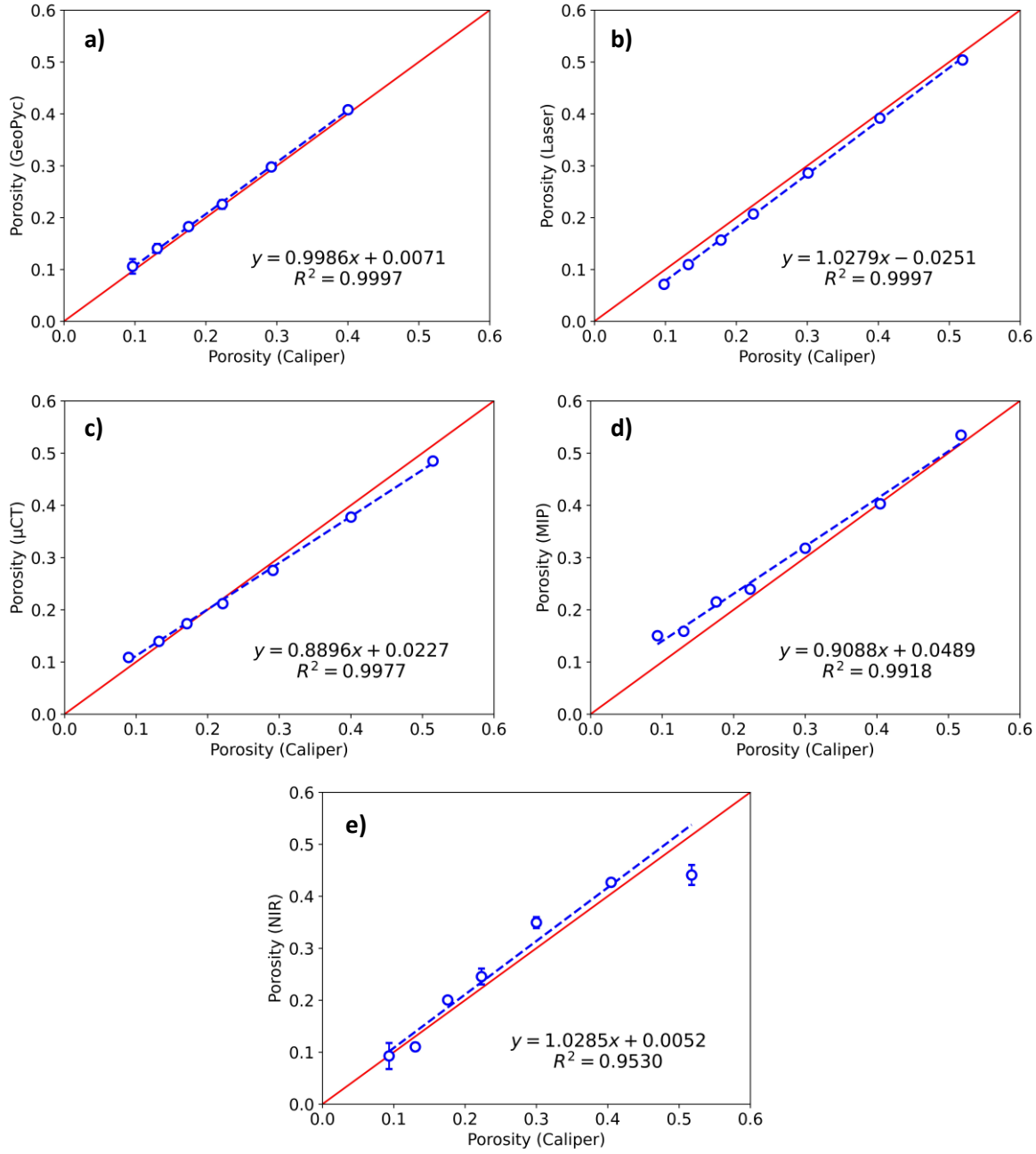

Figure 2. Comparison of five porosity measurement techniques to the Caliper method a) GeoPyc method, ribblets prepared at ~8 MPa were excluded from this test due to its low mechanical strength; b) Laser method; c) µCT; d) MIP, and e) NIR method. Except for MIP, error bars in both x and y directions are presented but some are hidden by the symbols. The solid red line in each figure is the line of identity.

good accuracy (p > 0.05 for slope = 1 and intercept close to 0) and precision (small error bar for both slope and intercept), indicating excellent agreement with that of the Caliper method (Figure 2a). The off-line NIR had large error bars for both slope and intercept. Therefore, despite a lack of statistically significant difference, its accuracy and precision are poorer. The other three methods showed significant differences to Caliper results for both slope and intercept. The Laser method demonstrated slightly lower accuracy (p < 0.05 for both slope and intercept), but good precision (small error bars for both slope and intercept). Both μCT and MIP had relatively lower accuracy, but μCT exhibited slightly better precision (smaller error bars) than MIP.

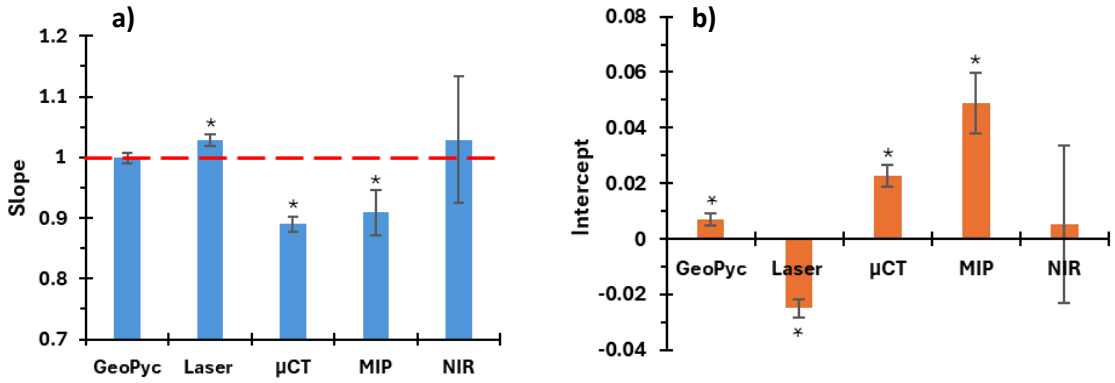

Figure 3. Results from the ODR analysis for five different measurement techniques, a) slope of the equation, b) intercept of the equation. Asterisk (*) indicates significant difference (p < 0.05) from 1 for the slope and from 0 for the intercept.

The accuracy of GeoPyc measurement also depends on three factors: 1) correct conversion factor (in cm^3/mm) that converts a change in displacement of the piston position (in mm) to a change in powder volume (in cm^3), 2) sample shape and size, and 3) sufficient sample volume percentage in the final powder bed, where ⩾25% of the final bed volume was recommended in the instrument manual (Micromeritics, 2013).

A theoretical value for the conversion factor can be calculated from the diameter of the chamber, which is 0.5065 cm^3/mm for a 25.4 mm diameter chamber. However, calibration for each measurement chamber is strongly recommended to ensure accuracy of measured values (Micromeritics, 2013). A default value of 0.5153 cm^3/mm for the test chamber used in this work was provided by the manufacturer. However, calibration performed using ribblets prepared at ~130 MPa yielded a conversion factor of 0.5067 cm^3/mm, which is close to the theoretical value but lower than the default value. If the default value (0.5153 cm^3/mm) were used, the measured volume by GeoPyc would result in a higher porosity (Figure S1). The impact of sample shape

and size on measured porosity is clearly seen in Figure 4, where cylindrical tablets with different thicknesses prepared under different pressures were used. Here, porosity of all cylindrical tablets measured by GeoPyc is higher than that by the Caliper method. In addition, the deviation tends to be larger for thinner tablets (i.e., higher surface area/volume ratio). Furthermore, even when an accurate conversion factor is used and sample size and shape have been kept unchanged, precision of measured porosity by GeoPyc is still affected by total sample volume. For example, when a single ribblet with a porosity of ~0.09 by Caliper method and volume ~4% of the final bed volume was measured by GeoPyc, RSD of 9 consecutive porosity measurements was 26.6%. However, RSD was reduced to 9.7% when the total sample volume was 20-25% of the final powder bed volume (Figure S2). Hence, it is critical to maintain sample volume to be sufficiently large, as suggested by the instrument manufacturer (Micromeritics, 2013), to ensure more precise and accurate ribbon porosity results by GeoPyc.

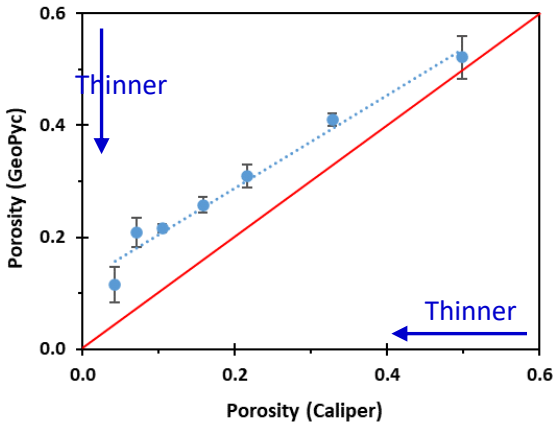

Figure 4. Porosity of cylindrical tablets (diameter of 11.28 mm) with the same weight but different thicknesses (2.5 - 4.7 mm) measured by GeoPyc method (conversion factor is 0.5067 cm^3/mm) and the Caliper method. The red solid line is the line of identity.

In summary, the good agreement between the GeoPyc measurement and the Caliper method in this portion of the study (Figures 2a & 3) is attributed to a) the use of an accurate conversation factor, determined using samples with nearly identical dimensions and physical presentations (ribblets prepared at ~130 MPa) to the testing samples, and b) the use of sufficient sample to attain 20-25% volume of the final powder bed.

Compared to the GeoPyc method, the Laser method directly measures the sample envelop volume through the scanning of sample's contour by the lasers (Iyer et al., 2014; Lillotte

et al., 2021; SolidFraction). The Laser method yielded porosity values slightly lower than that by the Caliper method (Figure 2b). The absolute difference is greater for ribblets compressed at a higher pressure. This may be due to the tablet flashing phenomenon (Paul et al., 2017) that leads to overestimated porosity by the Caliper method, which is to a higher extent for tablets compressed at a higher pressure. The precision of the Laser method is good, as suggested by the small error bars for both the slope and intercept of the ORD regression (Figure 3) and the small standard error for each measurement (Table S1). This observation is consistent with the observed in a previous study (Lillotte et al., 2021).

One advantage of the Laser method is its fast measuring speed, which is only 15 s from loading sample to reporting the results by the instrument (SolidFraction) (Table 1). Moreover, compared to the Caliper method, the Laser method is adaptable for samples with patterned and curved surfaces, typically encountered in ribbons manufactured during RC. These make it a possible process analytical technology (PAT) tool to monitor stability of RC process or guide RC process optimization (Lillotte et al., 2021). It is worth noting that as an envelope volume measurement technique, e.g., the Laser method and the GeoPyc method cannot detect internal cracks or distribution of pores within a sample. This limitation should be taken into account when measuring samples with such internal features (Lillotte et al., 2021).

Compared to the envelop volume measurement methods, such as the Caliper, GeoPyc, and Laser methods, the μCT can be used to map the density distribution within a sample and internal cracks and other defects in a sample can be excluded by the analyst (Lillotte et al., 2021). Thus, it exhibits distinct advantages when density distribution is not uniform, which is common in real ribbons, and when sample is in poor quality. In the current study, μCT method generated porosity values nearly identical to that by the Caliper method when porosity of ribblets was < 0.2. However, μCT porosity values were lower than the Caliper method for more porous ribblets (Figure 2c).

Porosity values from the MIP method also reasonably matched well with those by the Caliper method (Figure 2d). In contrast to the trend observed in the μCT data, deviation from the caliper data is greater with decreasing ribblet porosity. This may be attributed to the fact that the volume of pores smaller than 0.003 μm diameter were ignored in the method. Errors caused by this approximation had no detectable impact on measured values when porosity was > 0.4, but were more significant when porosity was < 0.4. An advantage of the MIP method is the ability to profile pore size distribution, in addition to the overall porosity. Although the MIP is effective in characterizing porous materials, good laboratory practices must be implemented to minimize any potential health risks by exposure to mercury.

307 The NIR method yielded reasonable predictions of porosity, which linearly correlates with
308 porosity measured by the Caliper method (Figure 2e). However, the correlation with the Caliper
309 method is weaker (R^2 = 0.9530) compared to other four methods ($R^{2>}$= 0.99).
310
311 **3.2. Ribbons from roller compactor**
312 Real ribbons are significantly different from the ribblets in terms of the physical presence.
313 Real MCC ribbons are irregular in shape, and slightly curved. The knurled pattern, uneven ribbon
314 thickness, and occasional defects due to cracks and ribbon splitting make the Caliper method
315 unfit for measuring ribbon porosity. In addition, the density distribution was not uniform for ribbons
316 prepared by RC. For example, ribbons prepared at 8.8 kN/cm exhibited clear non-uniform density
317 distribution, with center portion in darker color ("burnt"), indicating a higher density (Figure S4a).
318 NIR has been extensively studied as an off-line or in-line tool to determine or monitor the
319 porosity of ribbons prepared by RC (Acevedo et al., 2012; Khorasani et al., 2015b). While
320 performing well for intact ribbons with a smooth surface, the NIR technique encounters problems
321 with measuring porosity of broken, split, or curved ribbons. However, these practical issues facing
322 NIR technique for ribbon porosity measurement are rarely investigated (Crowley et al., 2017b).
323 Assessing the performance of the NIR method is further complicated by the fact that NIR only
324 measures local porosity at the region covered by the laser spot. If needed, this issue could be
325 mitigated by using multiple in-line NIR probes or measuring several spots in a sample using an
326 off-line NIR method.
327 Given the limitations with the Caliper method, only the Laser, μCT, GeoPyc, MIP and NIR
328 methods were compared for their performance in measuring porosity of real ribbons prepared at
329 two specific roll forces (1.8 kN/cm and 8.8 kN/cm). In the ribblet study, although GeoPyc provides
330 highest accuracy because of the strictly controlled dimensions and physical presences of the
331 calibration sample and the testing samples, the accuracy of the GeoPyc results is expected to
332 decrease when measuring irregular RC ribbon pieces. Ribblet porosity values measured by the
333 Laser method were close to the Caliper method while exhibiting higher precision than other
334 methods. Therefore, the laser porosity values were used as a reference for assessing the
335 performance of other methods in the RC ribbon measurements.
336 In the RC ribbon study, the conversion factor of 0.5067 cm^3/mm obtained from the ribblets
337 (~16 mm x 9 mm x 3 mm, L*W*H), was used in the GeoPyc method. Therefore, large RC ribbons
338 were broken into pieces with size closer to that of the ribblets for more accurate results. For μCT
339 analysis, the ROI spanned the entire ribbon width so that the average porosity is more
340 representative of the entire ribbon (Figure S6). The ROI along the length of ribbons (~10 mm)

was not precisely controlled, assuming negligible porosity variation along that direction for ribbons prepared under a steady state. For the NIR method, only "non-burned" area for 8.8 kN/cm ribbons were measured for the porosity evaluation. Therefore, the average porosity for the 8.8 kN/cm ribbon should have a lower value than that measured by NIR in Figure 5. The results indicate that, for ribbons compressed at 8.8 kN/cm, all other methods yield porosity values higher than that by the Laser method (Figure 5, Table S2). For the more porous ribbons made at 1.8 kN/cm, the GeoPyc methods yielded values closest to the Laser method, followed by the MIP method, the μCT method, and then the NIR method (Figure 5, Table S2).

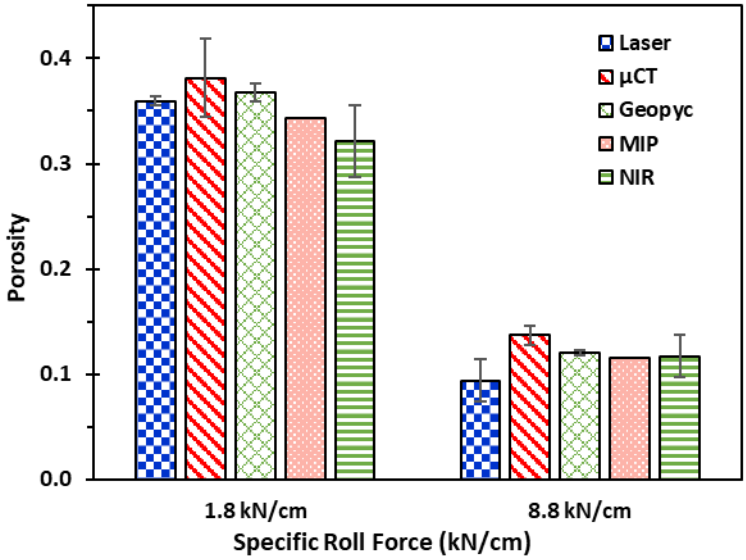

Figure 5. Relationship between porosity measured by the Laser method and 4 other techniques for ribbons prepared by roller compactor (n=3 for the Laser, μCT, and GeoPyc methods; n=2 for the MIP method; n=1 with 6 replicates for the NIR method). The blue dashed line is the line of identity.

3.3. Comparison among methods

The six methods were based on distinct physical principles for measuring different properties, e.g., envelope volume, density, pore volume (Table 1). They differ in sample requirement, where the Caliper method is most stringent as a simple geometry and smooth surface are essential for obtaining accurate sample volume. When such requirements are met, the Caliper method is a good choice as it is widely accessible, fast, and accurate. For irregular sample, other methods should be sought instead. The Caliper, Geopyc, and Laser methods only measure average porosity. Hence, they are not appropriate for samples that contain internal defects. In this regard, the MIP method holds advantages. However, the use of the MIP method

is limited by the potential health risks due to exposure to mercury, long measurement time, and less accessibility of an instrument. The sensitivity of GeoPyc to sample size and shape makes it more difficult to attain reproducible results, as it is not practical to demand similar shape and size between calibration sample and measurement samples. Compared to the GeoPyc method the Laser method is more flexible regarding sample shape and size, faster, and more repeatable. The μCT method is capable of modeling porosity distribution, instead of just measuring an average porosity. Thus, it provides more structural information of a ribbon, which may prove to be critical for understanding the RC process and guide its optimization. The NIR method does not generate porosity data as accurate as other methods, but its speed makes it suitable for in-line monitoring of a RC process, where detecting changes in ribbon properties is more important than measuring accurate porosity. In this regard, the Laser method also holds promise for potential PAT applications. Finally, both MIP and GeoPyc methods are destructive and require more extensive sample handling while applying stresses to samples during measurement. Thus, they are not suitable for fragile ribbon samples. In contrast, the non-destructive Laser, μCT, and NIR methods are suitable for fragile ribbon samples.

Table 1. Overview of the characteristics of six methods.

Method	Sample presentation	Measured property	Destructive ?	PAT?	Mapping ?	Total time[a]
Caliper	Simple shape, smooth surface	Envelop volume	N	N	N	30 s
GeoPyc	Shape and size Similar to samples used for calibration	Envelop volume	Y	N	N	20 min
μCT	No	Density	N	N	Y[1]	1 hr
NIR	Flat, smooth surface	Density	N	Y[2,3]	N	1 min
MIP	No	Porosity & Pore size distribution	Y	N	N	30 min
Laser	No (Length < 42 mm Thickness <8 mm, Width <10 mm)[4]	Envelop volume	N	Y[5,6]	N	15 s

[a] Estimated time includes sample preparation, data acquisition, data processing

References: 1.(Miguélez-Morán et al., 2009); 2,3 (Acevedo et al., 2012; Khorasani et al., 2015b); 4, (SolidFraction, 2022); 5,6 (Lillotte et al., 2021; Lück et al., 2024).

Results in this study confirm those in an earlier paper (Lillotte et al., 2021) when there is an overlap. The systematic comparison of six common methods for ribbon porosity determination lays a useful foundation for researchers to select most suitable methods for analyzing ribbons according to sample characteristics, desired accuracy and precision, speed, and information provided by each method.

4. Conclusion

Using ideal specimens, i.e., ribblets with a range of porosities prepared at different pressures on a compaction simulator, we found that the six methods produced globally similar ribbon porosity. Among them, the Caliper method is the most convenient and accessible for samples with a simple shape. However, this method is not suitable for real ribbons. The Laser method yielded data with accuracy and precision comparable to that from the Caliper method. The GeoPyc method gives reliable results for samples with regular shape, if appropriate conversion factor is used and the requirement of a sufficient sample volume percentage in the final powder bed is met. The μCT method yields more accurate results at lower porosities, while the MIP method yields more accurate results at higher porosities. The NIR method requires a calibration curve that covers the expected variability of the samples and a reliable sample presentation. Hence, while a promising non-destructive PAT tool for detecting changes in ribbons in real-time during a RC process, it is sensitive to several factors, such as composition variation, ribbons integrity, surface roughness, or flatness. Insights gained in this study can facilitate the choice of a suitable measurement method for characterizing ribbon porosity, which contributes to the optimization of ribbon quality and development of a robust tablet manufacturing process through dry granulation.

Acknowledgement

CCS thanks the National Science Foundation for support through the Industry University Collaborative Research Center (IUCRC) grant IIP-2137264, Center for Integrated Materials Science and Engineering for Pharmaceutical Products (CIMSEPP). YG thanks Gerrit Vreeman for ODR plotting and Vikram Joshi for discussions on the linear regression analysis.

References

Acevedo, D., Muliadi, A., Giridhar, A., Litster, J.D., Romañach, R.J., 2012. Evaluation of Three Approaches for Real-Time Monitoring of Roller Compaction with Near-Infrared Spectroscopy. AAPS PharmSciTech 13, 1005-1012.
Akseli, I., Iyer, S., Lee, H.P., Cuitiño, A.M., 2011. A Quantitative Correlation of the Effect of Density Distributions in Roller-Compacted Ribbons on the Mechanical Properties of Tablets Using Ultrasonics and X-ray Tomography. AAPS PharmSciTech 12, 834-853.
Allesø, M., Holm, R., Holm, P., 2016. Roller compaction scale-up using roll width as scale factor and laser-based determined ribbon porosity as critical material attribute. European Journal of Pharmaceutical Sciences 87, 69-78.
Athanasiou, L.S., Fotiadis, D.I., Michalis, L.K., 2017. Principles of Coronary Imaging Techniques. Academic Press, Oxford.
Bawuah, P., Markl, D., Farrell, D., Evans, M., Portieri, A., Anderson, A., Goodwin, D., Lucas, R., Zeitler, J.A., 2020. Terahertz-based porosity measurement of pharmaceutical tablets: a tutorial. Journal of Infrared, Millimeter, and Terahertz Waves 41, 450-469.
Berodier, E., Bizzozero, J., Muller, A.C., 2016. Mercury intrusion porosimetry, 1st Edition ed.
Boersen, N., Belair, D., Peck, G.E., Pinal, R., 2016. A dimensionless variable for the scale up and transfer of a roller compaction formulation. Drug Development and Industrial Pharmacy 42, 60-69.
Chang, S.-Y., Wang, C., Sun, C.C., 2019. Relationship between hydrate stability and accuracy of true density measured by helium pycnometry. International Journal of Pharmaceutics 567, 118444.
Crowley, M.E., Hegarty, A., McAuliffe, M.A., O'Mahony, G.E., Kiernan, L., Hayes, K., Crean, A.M., 2017a. Near-infrared monitoring of roller compacted ribbon density: Investigating sources of variation contributing to noisy spectral data. European Journal of Pharmaceutical Sciences 102, 103-114.
Crowley, M.E., Hegarty, A., McAuliffe, M.A.P., O'Mahony, G.E., Kiernan, L., Hayes, K., Crean, A.M., 2017b. Near-infrared monitoring of roller compacted ribbon density: Investigating sources of variation contributing to noisy spectral data. European Journal of Pharmaceutical Sciences 102, 103-114.
Donoso, M., Kildsig, D.O., Ghaly, E.S., 2003. Prediction of tablet hardness and porosity using near-infrared diffuse reflectance spectroscopy as a nondestructive method. Pharmaceutical development and technology 8, 357-366.
Elsergany, R.N., Vreeman, G., Sun, C.C., 2023. An approach for predicting the true density of powders based on in-die compression data. International journal of pharmaceutics 637, 122875.
Goldenberg, M., Vreeman, G., Sun, D.J., Moffit, M., Li, M., Zernik, M., Ahuja, S., Kim, Y., Semin, D., Sun, C.C., 2023. A material-sparing simplified buoyancy method for determining the true density of solids. International Journal of Pharmaceutics 635, 122694.
Iyer, R.M., Hegde, S., Singhal, D., Malick, W., 2014. A novel approach to determine solid fraction using a laser-based direct volume measurement device. Pharmaceutical development and technology 19, 577-582.
Keizer, H.L., 2021. title.
Keizer, H.L., Kleinebudde, P., 2020. Elastic recovery in roll compaction simulation. International Journal of Pharmaceutics 573, 118810.
Khorasani, M., Amigo, J.M., Bertelsen, P., Sun, C.C., Rantanen, J., 2016. Process optimization of dry granulation based tableting line: Extracting physical material characteristics from granules, ribbons and tablets using near-IR (NIR) spectroscopic measurement. Powder Technology 300, 120-125.
Khorasani, M., Amigo, J.M., Sonnergaard, J., Olsen, P., Bertelsen, P., Rantanen, J., 2015a. Visualization and prediction of porosity in roller compacted ribbons with near-infrared chemical imaging (NIR-CI). Journal of pharmaceutical and biomedical analysis 109, 11-17.

Khorasani, M., Amigo, J.M., Sun, C.C., Bertelsen, P., Rantanen, J., 2015b. Near-infrared chemical imaging (NIR-CI) as a process monitoring solution for a production line of roll compaction and tableting. European Journal of Pharmaceutics and Biopharmaceutics 93, 293-302.
Lillotte, T.D., Bebernik, P., Keck, J., Bommer, M., Schröder, D., Wagner, K.G., 2021. Laser triangulation as a fast and reliable method for determining ribbon solid fraction; focus on accuracy, precision, and measurement time. International Journal of Pharmaceutics 610, 121241.
Lim, H., Dave, V.S., Kidder, L., Neil Lewis, E., Fahmy, R., Hoag, S.W., 2011. Assessment of the critical factors affecting the porosity of roller compacted ribbons and the feasibility of using NIR chemical imaging to evaluate the porosity distribution. International Journal of Pharmaceutics 410, 1-8.
Lu, P., Lannutti, J.J., Klobes, P., Meyer, K., 2000. X-ray Computed Tomography and Mercury Porosimetry for Evaluation of Density Evolution and Porosity Distribution. Journal of the American Ceramic Society 83, 518-522.
Lück, M., Klinken, S., Kleinebudde, P., 2024. Laser Triangulation Based In-Line Elastic Recovery Measurement for the Determination of Ribbon Solid Fraction in Roll Compaction. Journal of Pharmaceutical Sciences 113, 1020-1028.
Mahmah, O., Adams, M.J., Omar, C.S., Gururajan, B., Salman, A.D., 2019. Roller compaction: Ribbon splitting and sticking. International Journal of Pharmaceutics 559, 156-172.
Micromeritics, 2013. GeoPyc 1365 Envelope Density Analyzer.
Miguélez-Morán, A.M., Wu, C.-Y., Dong, H., Seville, J.P.K., 2009. Characterisation of density distributions in roller-compacted ribbons using micro-indentation and X-ray micro-computed tomography. European Journal of Pharmaceutics and Biopharmaceutics 72, 173-182.
Nesarikar, V.V., Patel, C., Early, W., Vatsaraj, N., Sprockel, O., Jerzweski, R., 2012. Roller compaction process development and scale up using Johanson model calibrated with instrumented roll data. International journal of pharmaceutics 436, 486-507.
Osei-Yeboah, F., Sun, C.C., 2015. Validation and applications of an expedited tablet friability method. International Journal of Pharmaceutics 484, 146-155.
Paul, S., Chang, S.-Y., Sun, C.C., 2017. The phenomenon of tablet flashing — Its impact on tableting data analysis and a method to eliminate it. Powder Technology 305, 117-124.
Pawar, P.P., 2011. Measurement of mass and linear attenuation coefficients of gamma-rays of AL for 514, 662 and 1280 keV photons. J Chem Pharm Res 3, 899-903.
Reimer, H.L., Kleinebudde, P., 2019. Hybrid modeling of roll compaction processes with the Styl'One Evolution. Powder technology 341, 66-74.
Richards, F., Lindley, P., 2006. Determination of the density of solids. International tables for crystallography 100, 156-159.
SolidFraction, The New Solid Fraction Rapid Analyzer.
SolidFraction, 2022. Solid Fraction Rapid Analyzer Brochure
Souihi, N., Reynolds, G., Tajarobi, P., Wikström, H., Haeffler, G., Josefson, M., Trygg, J., 2015. Roll compaction process modeling: Transfer between equipment and impact of process parameters. International Journal of Pharmaceutics 484, 192-206.
Sun, C., 2004. A novel method for deriving true density of pharmaceutical solids including hydrates and water-containing powders. Journal of pharmaceutical sciences 93, 646-653.
Sun, C., 2005. True Density of Microcrystalline Cellulose. Journal of pharmaceutical sciences 94, 2132-2134.
Sun, W.-J., Rantanen, J., Sun, C.C., 2018. Ribbon density and milling parameters that determine fines fraction in a dry granulation. Powder Technology 338, 162-167.
Washburn, E.W., 1921. The dynamics of capillary flow. Physical review 17, 273.
Yu, L.X., Amidon, G., Khan, M.A., Hoag, S.W., Polli, J., Raju, G.K., Woodcock, J., 2014. Understanding pharmaceutical quality by design. The AAPS journal 16, 771-783.

Zhang, J., Pei, C., Schiano, S., Heaps, D., Wu, C.-Y., 2016. The application of terahertz pulsed imaging in characterising density distribution of roll-compacted ribbons. European Journal of Pharmaceutics and Biopharmaceutics 106, 20-25.
Zinchuk, A.V., Mullarney, M.P., Hancock, B.C., 2004. Simulation of roller compaction using a laboratory scale compaction simulator. International journal of pharmaceutics 269, 403-415.